Bull. Astr. Soc. India (2012) **40**, 213–241

Infrared emission from novae

A. Evans[1]* and R. D. Gehrz[2]†

[1]*Astrophysics Group, Lennard Jones Laboratory, Keele University, Keele, Staffordshire, ST5 5BG, UK*
[2]*Minnesota Institute for Astrophysics, School of Physics & Astronomy, 116 Church Street SE, University of Minnesota, Minneapolis, MN 55455, USA*

Received 2012 August 16; accepted 2012 October 28

Abstract. We review infrared observations of classical and recurrent novae, at wavelengths $> 3\,\mu$m, including both broad-band and spectroscopic observations. In recent years infrared spectroscopy in particular has revolutionised our understanding of the nova phenomenon, by revealing fine-structure and coronal lines, and the mineralogy of nova dust. Infrared spectroscopic facilities that are, or will be, becoming available in the next 10–20 years have the potential for a comprehensive study of nova line emission and dust mineralogy, and for an unbiased assessment of the extragalactic nova populations.

Keywords : classical novae – recurrent novae – infrared observations – circumstellar matter

1. Introduction

In many ways the 1970s marked the beginning of a golden age in our understanding of the nova phenomenon, as in this decade ultraviolet (UV) and infrared (IR) observations became available to complement the already well-observed (if not fully understood) optical observations. Indeed, it can be argued that this pan-chromatic view of the nova phenomenon was (as in many other areas of astrophysics) the key to understanding the bigger picture.

The IR window on novae was opened by the seminal observations by Geisel, Kleinmann & Low (1970), who obtained broadband photometric observations of Nova Serpentis 1970 (FH Ser) from 1–25 μm. The sharp rise in the flux longward of $\sim 2\,\mu$m, coinciding with the deep decline in the visual light curve, finally confirmed a hypothesis that had been gathering dust (so to speak)

*email: a.evans@keele.ac.uk
†email: gehrz@astro.umn.edu

since 1935. In 1934 the nova DQ Her – one of the best observed novae of all time – erupted and displayed a deep ($\gtrsim 10$ mag) minimum in the visual light curve (see Martin (1989a) for a schematic light curve, based on AAVSO observations). With extraordinary insight, McLaughlin (1935) suggested that the deep minimum might have arisen as a result of the formation of dust in the material ejected in the 1934 eruption, but the technology to make the IR observations required to confirm the dust hypotheses did not exist at the time.

The pan-chromatic view of the nova phenomenon has shown that the circumstellar environment of an erupting nova is extraordinarily hostile, not conducive to the chemistry required to go from a plasma, via small molecules to dust grains. An alternative proposal to dust formation was proposed by Bode & Evans (1980), who suggested that the dust giving rise to the IR emission pre-dates the eruption, by producing an "infrared echo". However, with one or two exceptions – in which there is clear evidence for such "pre-existing" dust – it now seems clear that chemistry and dust-formation do indeed proceed in the winds of erupting novae. The coincidence of the minimum in the visual light curve and rise in the IR, as the newly-formed dust reradiates the absorbed visual light, is well illustrated in the case of the novae NQ Vul (Ney & Hatfield 1978) and LW Ser (see Fig. 1; Gehrz et al. 1980). This is now regarded as irrefutable evidence that the dust forms in the newly-ejected material.

However there is more to IR observations of novae than the detection and characterisation of dust. As the eruption proceeds, from the expanding fireball, through the free-free phase, to the nebular and (in some cases) coronal phases, the ionisation and excitation of the dispersing ejecta by the still-hot white dwarf results in a rapidly evolving emission line spectrum. The continuum (free-free) emission can be used to estimate the ejected mass, while the emission lines can be used to determine elemental abundances in the ejecta if the state of the still-hot central engine is known. In the case of fine-structure and coronal emission, abundances can in some cases be determined using relatively simple atomic physics.

In this contribution we review the IR properties of classical and recurrent novae at wavelengths longward of $\sim 3\,\mu$m; a companion paper in this issue (Banerjee & Ashok 2012) is devoted to IR observations of novae shortward of $3\,\mu$m.

2. The nova phenomenon: some context

As is well known (see Bode & Evans 2008, for a recent review), a nova explosion occurs in a semi-detached binary system in which a white dwarf (WD) accretes material from a cool star via an accretion disc. The base of the accreted material is compressed and heated, and becomes (electron) degenerate. A Thermonuclear Runaway (TNR) eventually occurs and, as degeneracy is lifted, the accreted material is ejected in a nova explosion. Mass transfer then resumes and in time further nova explosions occur; this may be on a timescale $\sim 10^4 \ldots 10^5$ years (a classical nova), or on a human timescale, $\lesssim 100$ years (a recurrent nova). Indeed, it may be that the recurrence time is not so markedly bimodal, and that there is a spectrum of recurrence times, which has not

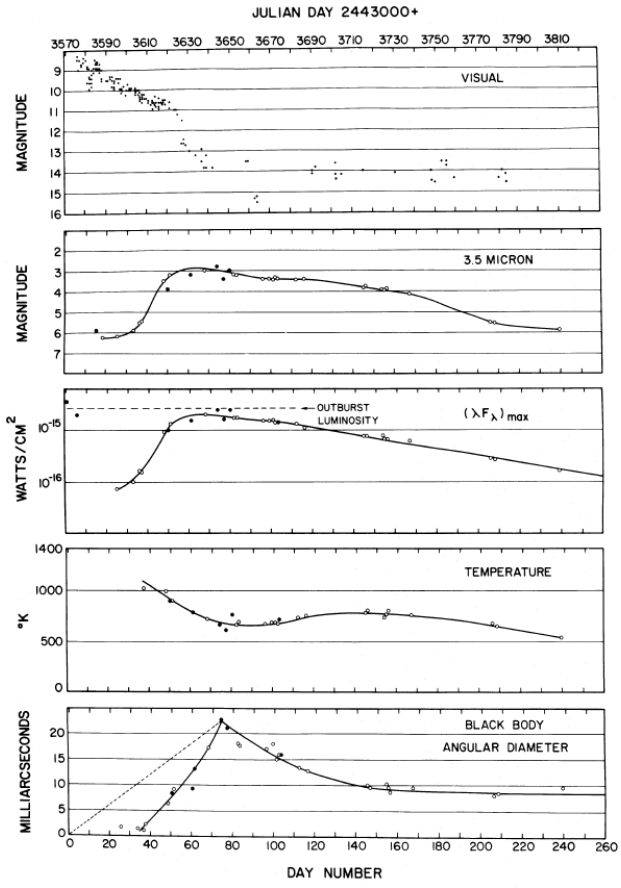

Figure 1. Optical and IR development of the dusty nova LW Ser. From top to bottom: visual light curve from AAVSO data; 3.5 μm light curve; optical-IR luminosity, as measured by $\{\lambda f_\lambda\}_{\max}$, where f_λ is the flux density in wavelength units; black body temperature of the dust; black body angular diameter. See Gehrz et al. (1980) for details.

yet become manifest. In any case, whether a classical or a recurrent, a nova system undergoes many eruptions.

In the course of the explosion some 10^{-5} to $10^{-4}\,M_\odot$ of material is ejected, at speeds ranging from a few hundred to several thousand $\mathrm{km\,s^{-1}}$. By virtue of the fact that the explosion has its origin in a TNR the ejected material is enriched in CNO (and other elements). Some species observed in nova ejecta are unlikely to have been generated in the TNR, and it is clear that some of the WD must be dredged up into the accreted material, as first suggested by Ferland & Shields (1978b) to account for the large neon over-abundance in V1500 Cyg. This led to the realisation that the compact object in the nova binary may be either be a CO WD or a more massive ONe WD.

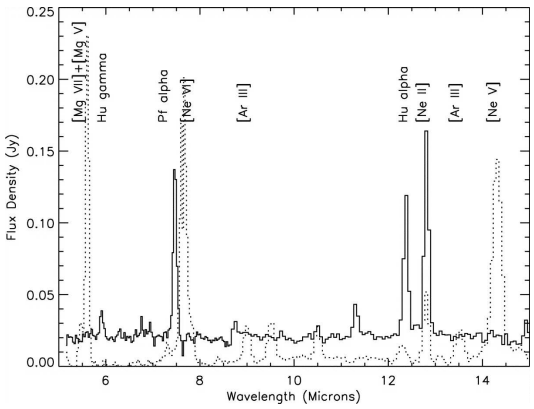

Figure 2. The contrast between the strength of the neon lines in a CO nova V1186 Sco (solid line) and a neon nova (dotted line) (Schwarz et al. 2007).

Nova eruptions on the former tend to have ejecta masses at the lower end of the mass range and to be the prolific dust producers, while novae in systems containing ONe WD tend to be faster – as the violence of the explosion depends on the WD mass – eject higher masses, and seem generally incapable of forming much dust. Nova explosions on ONe WD are often termed "neon novae", on account of the great strength of neon lines in their optical and IR spectra; novae originating on CO WDs are termed "CO novae". The differences in their spectra over the wavelength range $5 - 15\,\mu$m, where there are a number of neon lines, are well illustrated (see Fig. 2) in the cases of V1186 Sco (a CO nova) and V1187 Sco (a neon nova).

The energetics of a nova explosion are well parametrised by the time t_2 (or t_3) that the nova's visual light curve takes to decline by 2 (or 3) magnitudes from maximum, although the (extremely) erratic nature of some nova light curves makes this parameter not only difficult to determine but also to define. Faster novae (i.e. smaller t_2) have greater bolometric luminosities and ejection velocities. A key point is that fact that the bolometric luminosity remains constant throughout the early part of the eruption (the TNR "switches off" after about 1…10 years; see Krautter 2008) and so as the mass-loss declines, the effective temperature of the stellar remnant increases as the pseudophotosphere collapses back onto the WD (Bath & Harkness 1989). This has implications for the evolution of both the line and dust emission.

3. Broad-band IR observations

The earliest IR observations consisted of broad-band photometry, most often in the *JHKL* (and sometimes *M*) bands[1], but also at longer wavelengths. Despite the limitations of broad-band observations, they were key to revealing three important aspects of the nova phenomenon: the

[1] $J = 1.25\,\mu$m, $H = 1.65\,\mu$m, $K = 2.2\,\mu$m, $L = 3.5\,\mu$m, $M = 4.8\,\mu$m

formation of dust, the presence of spectral features in the IR, and the determination of the ejected mass.

As already mentioned, some of the early broad-band observations revealed the condensation of significant quantities of dust in the ejected material (e.g. Geisel et al. 1970; Ney & Hatfield 1978; Gehrz et al. 1980). However even now, more than 40 years on, the very rapid grain growth in novae remains a poorly understood aspect of the dust formation process. For example, in the proto-typical heavy dust formers such as V705 Cas (Mason et al. 1998; Evans et al. 2005) and LW Ser (see Fig. 1; Gehrz et al. 1980), the grains grow to maximum size (typically $\sim 1\,\mu$m) as judged from the optical extinction event, in only 20–40 days. The inference is that grains grow with extremely high efficiency once they have nucleated. A possible mechanism has been proposed by Shore & Gehrz (2004), who argued that photo-ionisation of condensates by the hard radiation field of the central engine can induce runaway grain growth. Dust formation may also be facilitated by the clumpiness of nova ejecta, and the fact that the cores of the clumps are shielded from the hardest radiation. H-α and thermal IR images of the circum-binary ring around the hot, luminous, over-contact binary RY Sct clearly demonstrate that dust can form behind an ionisation front that has blocked the ionising photons from the dust formation zone (Smith, Gehrz & Goss 2001; Smith et al. 2011).

The nature of the broad-band data meant that little could be deduced about the nature of the dust, although the expected overabundance of CNO elements in the ejecta hinted at carbon. As the bolometric luminosity $L_{\rm bol}$ of the nova remains constant during the early eruption (predicted by the TNR model of the nova eruption, and confirmed by multi-wavelength observations) a simple interpretation gives

$$t_{\rm c} = \left(\frac{L_{\rm bol} Q_*}{16\pi v^2 \sigma A T_{\rm c}^{(\beta+4)}} \right)^{1/2}$$

for the dust condensation time $t_{\rm c}$, in terms of the ejecta speed v and condensation temperature $T_{\rm c}$. The parameters A and β are defined such that the IR emissivity of the dust is $= A\,\{c/\lambda\}^{\beta}$, and Q_* is the absorptivity of the dust, averaged over the spectral energy distribution (SED) of the stellar remnant.

As the dust flows away from the site of the explosion, the dust temperature $T_{\rm d}$ is expected to decline with time t as $T_{\rm d} \propto t^{-2/(\beta+4)}$ but in some particularly dusty novae (such as NQ Vul), the dust temperature remains roughly constant with time (see e.g. Ney & Hatfield 1978; Gehrz et al. 1980, this is well illustrated in Fig. 1 for LW Ser) – the so-called "isothermal" stage – indicating that the dust physics is rather more complex than indicated above. However as noted by Evans & Rawlings (1994) the luminosity as seen by the grains is not constant, because of the way in which ionisation fronts sweep through the ejecta. The isothermal phase has been interpreted in terms of grain destruction, by chemisputtering of carbon grains (Mitchell & Evans 1984; Mitchell, Evans & Albinson 1984), and the photo-processing of carbon dust (Evans & Rawlings 1994). Indeed, the chemisputtering of amorphous carbon dust by hydrogen led Mitchell & Evans (1984)

to predict the presence of aromatic infrared (AIR)[2] features in novae, subsequently discovered in V842 Cen (Hyland & McGregor 1989) and V705 Cas (Mason et al. 1998; Evans et al. 2005, see Section 4.2.3 below).

Broad-band observations were also sufficient to hint at the presence of the CO molecule early in the IR development of NQ Vul (e.g. Gehrz, Hackwell & Briotta 1976; Ney & Hatfield 1978); the bandhead of the CO fundamental vibrational transition is at 4.6 μm, which elevates the $M-$band flux. Indeed the data presented by Gehrz et al. (1976) clearly show that lines (probably the CO bandhead) contributing to the 5 μm excess were present before the dust formed. This molecule is key to understanding the chemistry that leads to dust formation. While the conventional paradigm is that the C:O ratio (by number) in the ejected material determines the nature of the dust formed, this assumes that CO formation goes to saturation so that whichever of C and O has the lower abundance is locked up in CO; this seems not to apply to nova ejecta, in which CO formation does not go anywhere near saturation, giving rise to the production of a variety of dust types. An alternative explanation for the latter is that there are strong abundance gradients within the ejecta.

Early broad-band observations also hinted at the presence of the [Ne II]12.81 μm fine-structure line, in the IR observations of V1500 Cyg (Ennis et al. 1977; Ferland & Shields 1978a), giving rise (as noted above) to the neon nova concept. As we discuss below, the IR fine-structure (and coronal) lines provide a means of estimating ejecta temperature and abundances.

The mass ejected ($M_{\rm ej}$) in a classical nova eruption is a key parameter. It is central to the understanding of the TNR, to the determination of abundances, and to the contribution that novae make to the chemical evolution of the Galaxy (see e.g. Bode & Evans 2008, and chapters and references therein, for a full discussion of ejected masses). It is also key to the fate of the WD in the nova system. If $M_{\rm ej}$ is less than the mass accreted by the WD then the mass of the latter must increase with time, with implications for a potential link between nova systems and the progenitors of Type Ia supernovae; but if $M_{\rm ej}$ exceeds the accreted mass then novae are likely greater contributors to Galactic chemical evolution than hitherto thought. Either way this one parameter lends novae a great significance in the bigger picture.

The ejected mass may be determined by multi-wavelength broad-band IR observations during the free-free phase; the observations fix the wavelength $\lambda_{\rm c}$ at which the free-free emission becomes optically thick, a measure of the shell density (see Gehrz 2008, and references therein). Masses can also be determined using a Thomson scattering model when IR observations show that the fireball is becoming optically thin (Gehrz 2008). Ejected masses determined by these two methods agree when applied to the same nova and are typically in the range $0.5 - 10 \times 10^{-5}$ M$_\odot$ (see Gehrz et al. 1998; Gehrz 2008, for a summary); ejected masses determined from radio observations are comparable (see Seaquist & Bode 2008, for a summary), although IR and radio ob-

[2]The aromatic and aliphatic hydrocarbon features seen in a wide variety of astrophysical sources – including novae – have been variously referred to as HAC features, PAH features, UIR features and AIR features; we use the latter designation here.

servations sample different regions of the ejected material (Gehrz 2008). These observationally-determined masses are significantly greater than those expected from the TNR theory (e.g. Starrfield, Iliadis & Hix 2008), and the discrepancy is all the greater when it is noted that neither IR nor radio observations include any neutral material.

4. IR spectroscopy

IR spectroscopy (with spectral resolution $R = \lambda/\Delta\lambda \gtrsim 50$) became widespread in the 1980s and it is at this time that IR observations of novae began to rival optical observations in their diagnostic capability. In particular spectroscopic observations from observatories in space, especially the *Infrared Space Observatory* (*ISO*; Kessler et al. 1996) and more recently the *Spitzer Space Telescope* (Werner et al., 2004; Gehrz et al. 2007), have been pivotal in advancing our understanding of the circumstellar environments of novae.

4.1 Line emission

As is well known, when the visual light curve has declined by about 3 magnitudes, the optical spectrum of a classical nova makes the dramatic "transition" from absorption to emission (see Payne-Gaposchkin 1957, for a very nice illustration of this in the case of DQ Her). Much else happens around this time, such as the formation of dust in the ejected material. Thereafter, the ionisation states of the emission lines increase as the pseudophotosphere collapses onto the white dwarf (see above), with specific ionisation states appearing at well-defined epochs in the evolution of the eruption (see Bath 1978, especially Fig. 5, for an early discussion of this point). As the nova eruption progresses, a number of fine-structure lines appear longward of $3\,\mu$m and, in some cases, coronal lines appear as well.

4.1.1 *The nebular phase*

The evolution of the nebular spectrum of novae is well observed and hydrogen recombination lines appear very early in the development of the nebular spectra; prominent series with lines in the wavelength range of the *Spitzer* Infrared Spectrograph (IRS; Houck et al. 2004) include the Humphreys ($n \rightarrow 6$, $\lambda_\alpha = 12.37\,\mu$m), $n \rightarrow 7$ ($\lambda_\alpha = 19.06\,\mu$m) and $n \rightarrow 8$ ($\lambda_\alpha = 27.80\,\mu$m) series, where n is the principal quantum number of the upper level.

The nebular phase offers the potential to determine elemental abundances in the ejected material (and hence of the material produced in the TNR). However the determination of abundances can be fraught with difficulties, including (a) the poorly known interstellar extinction (and its wavelength-dependence) to novae in general, (b) the possible wavelength dependence of any circumstellar extinction (but in the case of V705 Cas this was known to be neutral, at least in the UV; Shore et al. 1994), (c) the clumpiness of nova ejecta, and (d) the physical state of the ionising

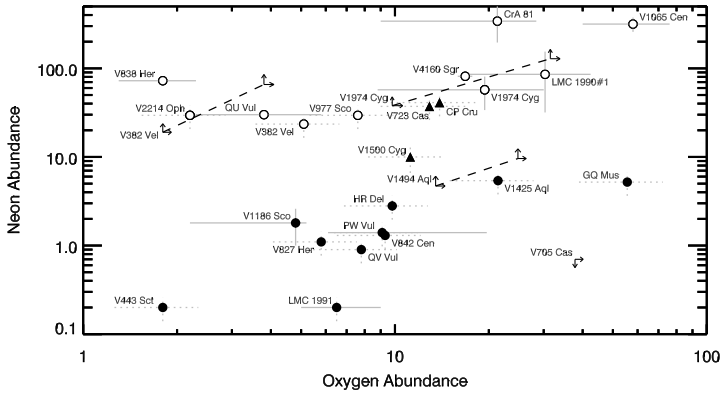

Figure 3. Neon over-abundances versus oxygen over-abundances (in both cases relative to solar) for a variety of recent novae. The open circles represent the ONe targets, the filled circles represent the CO novae, and the filled triangles are atypical novae. It is clear that the strong dust formers fall in the regime where the neon abundance is 1–5 times solar, and that the neon novae have neon abundances that are much higher than solar. From Helton et al. (2012); see this paper for further details.

and/or exciting mechanism. In general, the ejected material is likely to be highly asymmetric (e.g. displaying equatorial rings and polar caps) and to have abundance gradients.

However, longward of 3 μm the reddening becomes a lesser issue, and observations with the *Spitzer* IRS have played a prominent role in the determination of elemental abundances in nova ejecta. Determinations of nebular abundances generally make use of well-tested photoionisation codes such as CLOUDY (Ferland et al. 1998, and earlier papers), which necessarily make simplifying assumptions, e.g. regarding the geometry of the ionised material, although NEBU (Morriset, Stasińska & Peña 2005) allows for a range of nebular geometries. Given the prominence of hydrogen recombination (and other) lines it is relatively straight-forward to express abundances relative to H, and then compare this with an assumed solar abundance[3] (e.g. Asplund et al. 2009).

A summary of abundances in nova ejecta, including some values obtained with *ISO* and *Spitzer*, is given by Gehrz (2008), while compilations of abundances deduced using *ISO* and *Spitzer* data (as well as data at shorter wavelengths) are given by José & Shore (2008) and Helton et al. (2012). Caution should be exercised in comparing these abundances as they are expressed relative to differently-assumed solar abundances.

In Fig. 3, we show the relative abundances of neon and oxygen in nova ejecta, as determined from *ISO* and *Spitzer* observations, together with observations at shorter wavelengths (Helton et

[3]Care should be exercised in comparing nova abundances relative to solar as the latter are occasionally revisited; see José & Shore (2008) for a discussion of this point.

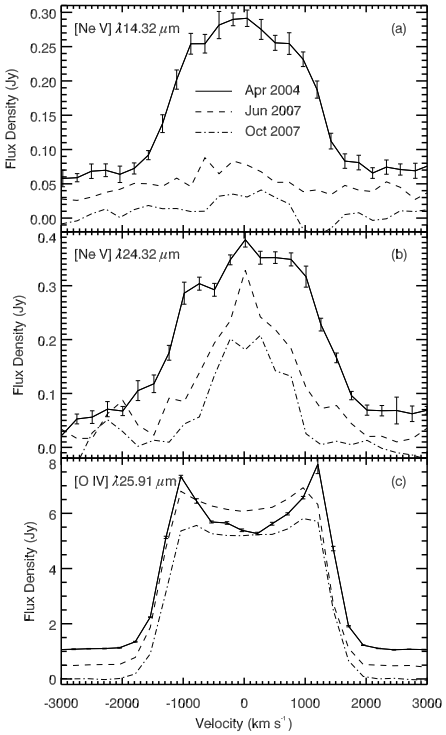

Figure 4. Line profiles for three fine-structure lines in the IR spectrum of V1494 Aql. Note the difference between the profiles of the neon and oxygen lines. From Helton et al. (2012).

al. 2012); note that the Ne abundance for QU Vul in this Figure is from Schwarz (2002) rather than the more recent determination by Gehrz et al. (2008). Also the abundances in this figure have been adjusted to a standard solar value. Note that the novae in this figure do not form a homogeneous sample: they are generally selected on the grounds that they happened to trigger a target-of-opportunity programme. However there is a clear demarcation between CO and neon novae, the latter having neon overabundance relative to solar of $\gtrsim 20$.

Line profiles during the nebular phase have long been known to be complex and this is also the case for IR emission lines. A selection of line profiles for V1494 Aql is shown in Fig. 4 (from Helton et al. 2012). The saddle-shaped profile of the [O IV]25.91 μm line resembles that of the optical emission lines seen early in the outburst, and indicates an equatorial cap/polar cap structure in the ejecta. The profiles of the neon lines, on the other hand, are less complex, and may indicate that the emission arises in a geometrically thick, but optically thin, shell (Helton et al. 2012). Such differences may indicate that these ions reside in different regions of the ejecta (this may also be suggested by the range of dust types formed in nova ejecta; see Section 4.2 below).

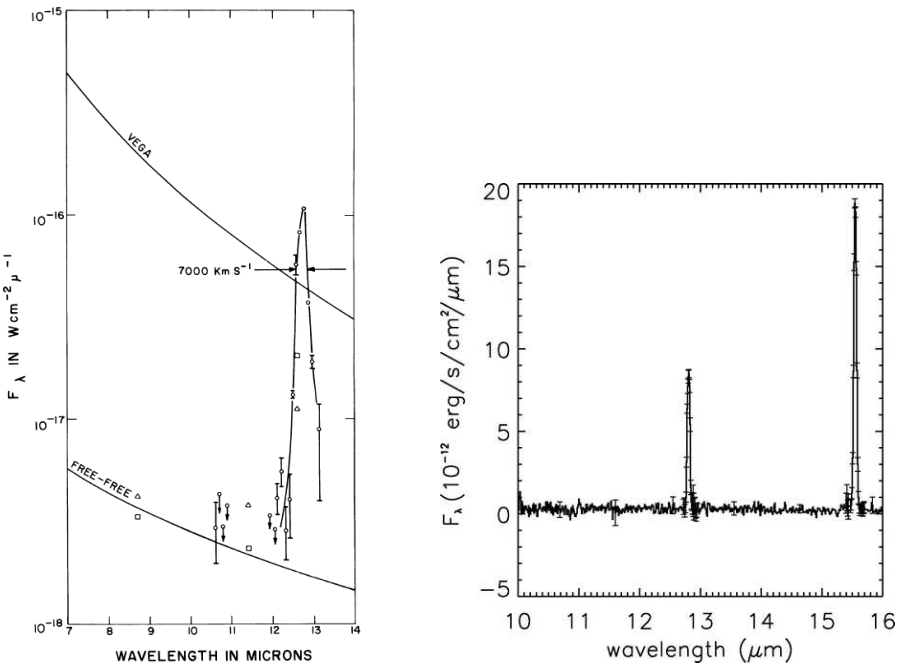

Figure 5. Left: Ground-based IR spectrum of QU Vul in the 8 – 13 μm window, showing free-free emission and strong emission in the [Ne II]12.81 μm fine-structure line. From Gehrz et al. (1985). Right: Spectrum of QU Vul in the same wavelength range using the *Spitzer* IRS (Gehrz et al. 2008).

4.1.2 *Fine structure emission*

The ground states of heavy elements may have fine structure having the same L and S quantum numbers but different J. The upper level is easily populated (usually by electron collision) and radiative de-excitation may then occur giving rise to fine structure line emission; the transitions are highly forbidden, and the upper level is collisionally de-exited if the electron density exceeds a specific value $n_{\rm crit}$. Such transitions may act as extremely efficient coolants in low density nebulae (see Ferland et al. 1984, who made an early prediction of the likely strength of [O IV]25.89 μm and other far-IR fine-structure lines in novae).

[Ne II] was the first IR fine-structure line to be observed in a nova (V1500 Cyg) and on this basis Ferland & Shields (1978a) suggested that both [Ne II]15.56 μm and [O IV]25.89 μm would also be strong. QU Vul (Fig. 5) was subsequently discovered to have the strongest [Ne II]12.8 μm relative to the continuum ever observed in an astrophysical source (Gehrz et al. 1985), thus becoming the "quintessential" example of a neon nova. [O IV] was subsequently found to be very prominent in the spectra of V1974 Cyg (Salama et al. 1996), V705 Cas (Salama et al. 1999) and V1425 Aql (Lyke et al. 2003) in data obtained with *ISO*; see also below. More recently observa-

tions of novae with the *Spitzer* IRS have also found prominent [O IV], and also [Ne II]12.81 μm, [Ne III]15.55 μm, [Ar III]8.99 μm and [S IV]10.51 μm (see Fig. 5).

The importance of these lines is that they may provide a relatively elementary estimate of the abundance of the emitting ion. The ion may be treated as a simple two-level system and detailed balance then requires that the total number of emitting ions N is

$$N = \frac{L\lambda}{n_e hc} \; \frac{1 + [n_e/n_{crit}]}{q_{12}}$$

where λ is the wavelength of the transition, L is the luminosity in the transition and q_{12} is the (temperature-dependent) collisional excitation rate (Gehrz et al. 2008). In the low density limit (i.e. $n_e \ll n_{crit}$), every collisional excitation is followed by a radiative de-excitation.

This technique has been used by Gehrz et al. (2008) to determine a lower limit on the neon abundance in the ejecta of the neon nova QU Vul. Fig. 5 shows the spectrum of this nova, obtained from the ground in the 8 – 13 μm window in 1984, 140 days after outburst (Gehrz et al. 1985), and in 2004 – over a similar wavelength range – with the *Spitzer* IRS. Strong emission in the [Ne II] fine structure line is evident, as is (in 2004) emission by [Ne III]15.55 μm. Gehrz et al. (2008) concluded that QU Vul was over-abundant in neon (relative to solar) by a factor of at least 168 some 19 years after eruption. Such large overabundances, combined with the observed ejected masses, suggest that novae are not insignificant contributors to the chemical evolution of the Galaxy.

A list of fine-structure lines longward of 3 μm expected to be observed in novae is given in Table 1, in which E.P and I.P. are respectively the excitation potential of the upper level and the ionisation potential needed to form the ion respectively. The list includes a number of lines that are commonly seen in the IR spectra of novae, such as [Ca IV]3.20 μm and [Ne II]12.81 μm. Also included are various sodium lines, such as [Na III]7.31 μm. ^{22}Na is predicted to be produced in the TNR, particularly on high-mass WDs. This isotope is radioactive and undergoes β^+−decay to ^{22}Ne with half-life 2.6027 years; this decay should be observable as the line spectrum evolves. However, while a number of neon lines are well-observed in the IR spectra of novae, the sodium lines have so far proved elusive.

In a careful and thorough discussion of the evolution of the emission line spectrum of DQ Her, Martin (1989a,b) has predicted the variation of the emission line fluxes from ~ 40 days to ~ 50 years after eruption, for emission lines in the UV, optical and IR/far-IR. With the caveat that this calculation is for the elemental abundances, physical conditions and the stellar remnant of DQ Her, the expected variation with time is shown in Fig. 6. Note that some lines, such as [Ne III]36.01 μm, decline significantly with time; others, such as [O IV]25.89 μm, are expected to remain strong for many years, even decades, after outburst. The observed strength of the [O IV] line is borne out by *ISO* and *Spitzer* observations of V1974 Cyg (Salama et al. 1996; Helton et al. 2012), V705 Cas (Salama et al. 1999), V1425 Aql (Lyke et al. 2001), CP Cru (Lyke et al. 2003), V1187 Sco (Lynch et al. 2006), QU Vul (Gehrz et al. 2008), V2362 Cyg (Lynch et al. 2008), DZ Cru (Evans et al. 2010), V1065 Cen (Helton et al. 2010), V328 Vel and V1494 Aql (Helton et al. 2012), and in the recurrent nova RS Oph (Evans et al. 2007b,c)

Table 1. Selected fine-structure lines with wavelength > 3 μm, from Lutz (2002).

Species	Transition	λ (μm)	E.P. (eV)	I. P. (eV)
[Ca IV]	$^2P_{1/2}-^2P_{3/2}$	3.2067	50.91	67.27
[Ca V]	$^3P^1-^3P^2$	4.1594	67.27	84.50
[Ar VI]	$^2P_{3/2}-^2P_{1/2}$	4.5295	75.02	91.01
[Na III]	$^2P_{1/2}-^2P_{3/2}$	7.3177	47.29	71.62
[Ar V]	$^3P_2-^3P_1$	7.9016	59.81	75.02
[Ar III]	$^3P_1-^3P_2$	8.9914	27.63	40.74
[Na IV]	$^3P_1-^3P_2$	9.0410	71.62	98.91
[S IV]	$^2P_{3/2}-^2P_{1/2}$	10.5105	34.79	47.22
[Ca V]	$^3P_0-^3P_1$	11.4820	67.27	84.50
[Ne II]	$^2P_{1/2}-^2P_{3/2}$	12.8136	21.56	40.96
[Ar V]	$^3P_1-^3P_0$	13.1022	59.81	75.02
[Ne III]	$^3P_1-^3P_2$	15.5551	40.96	63.45
[S III]	$^3P_2-^3P_1$	18.7130	23.34	34.79
[Na IV]	$^3P_0-^3P_1$	21.2900	71.62	98.91
[Ar III]	$^3P_0-^3P_1$	21.8302	27.63	40.74
[O IV]	$^2P_{3/2}-^2P_{1/2}$	25.8903	54.93	77.41
[S III]	$^3P_1-^3P_0$	33.4810	23.34	34.79
[Ne III]	$^3P_0-^3P_1$	36.0135	40.96	63.45
[O III]	$^3P_2-^3P_1$	51.8145	35.12	54.93
[N III]	$^2P_{3/2}-^2P_{1/2}$	57.3170	29.60	47.45
[O I]	$^3P_1-^3P_2$	63.1837	0.00	13.62
[O III]	$^3P_1-^3P_0$	88.3560	35.12	54.93

4.1.3 *Coronal emission*

A working definition of coronal emission is given by Greenhouse et al. (1990) as emission lines "arising from ground-state fine-structure transitions in species with ionisation potential (I.P.) > 100 eV". The distinction from fine structure lines is in the high energy needed to form the ions concerned. From the nova perspective, coronal emission was first observed optically in the recurrent nova RS Oph (see Wallerstein 2008, for a retrospective). Coronal lines are often observed in the IR spectra of novae, but not all novae undergo a coronal phase.

The high ionisation states observed in coronal emission may arise from photoionisation (e.g. novae are known X-ray emitters during and after eruption, Krautter 2008). Alternatively, they may be excited by collisional ionisation if there are strong shocks in the nova environment, either between ejecta moving at different speeds or by the interaction of ejected material with a pre-existing wind. The required strong interaction between ejecta and a stellar wind is well established in the case of the recurrent nova RS Oph (see Section 5 below). A list of actual and

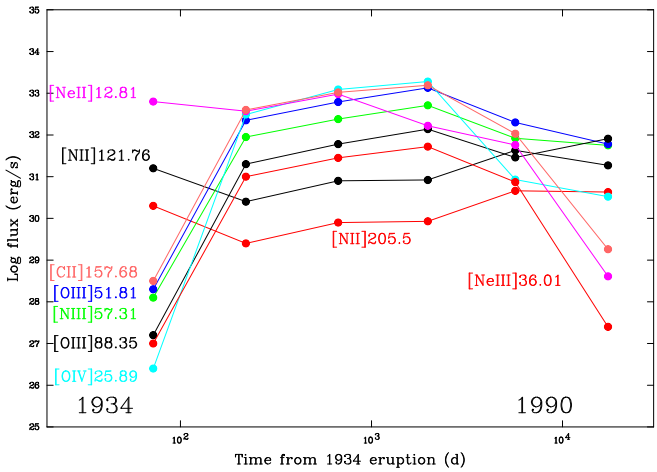

Figure 6. Predicted variation in fine structure line fluxes, over a period ~ 70 years, for DQ Her 1934. Based on Martin (1989b).

potential coronal lines longward of 3 μm that may be present in the IR spectra of novae is given in Table 2.

A discussion of IR coronal line emission in novae is given by Greenhouse et al. (1990). These authors use coronal line intensity ratios to determine that the electron temperatures in the coronal zones in novae are $\sim 3 \times 10^5$ K. Abundances are then estimated from individual line intensities and by summing over ionisation states; this latter step has to assume a specific form for the collisional ionisation equilibrium as a function of temperature. As noted by Greenhouse et al. (1990) the outcome is very dependent on the plasma model assumed.

4.2 Dust emission

As noted in Section 1 the idea of dust formation in nova winds has been around since the 1930s and it is now a well-observed phenomenon in the IR. A review of dust formation in novae is given by Evans & Rawlings (2008) and Gehrz (2008); see also José & Shore (2008).

There have been several attempts to correlate the dust-forming capabilities of novae with other parameters, such as speed class, outburst luminosity, ejected mass, and outflow velocity; see Gehrz & Ney (1987), Gehrz (1988) and Evans & Rawlings (2008) for discussions. However it is likely that whether or not a nova forms dust depends on the complex interaction between a number of parameters, but it is apparent from Fig. 3 that there is an anti-correlation between the presence of strong coronal lines and the nova's ability to form dust.

Table 2. Selected coronal lines (as defined by Greenhouse et al. 1990) with wavelength > 3 μm, from Lutz (2002). See text for definition of "coronal".

Species	Transition	λ (μm)	E.P. (eV)	I. P. (eV)
[Mg VIII]	$^2P^{3/2}$–$^2P^{1/2}$	3.0279	224.95	265.96
[Al VI]	$^3P_1$–$^3P_2$	3.6597	153.83	190.48
[Al VIII]	$^3P_2$–$^3P_1$	3.6900	241.44	284.60
[Si IX]	$^3P_1$–$^3P_0$	3.9357	303.17	351.10
[Ca VII]	$^3P_2$–$^3P_1$	4.0858	108.78	127.20
[Mg IV]	$^2P_{1/2}$–$^2P_{3/2}$	4.4867	80.14	109.24
[Na VII]	$^2P_{3/2}$–$^2P_{1/2}$	4.6847	172.15	208.44
[Mg VII]	$^3P_2$–$^3P_1$	5.5032	186.51	224.95
[Mg V]	$^3P_1$–$^3P_2$	5.6099	109.24	141.27
[Al VIII]	$^3P_1$–$^3P_0$	5.8500	241.44	284.60
[Ca VII]	$^3P_1$–$^3P_0$	6.1540	108.78	127.20
[Si VII]	$^3P_0$–$^3P_1$	6.4922	205.05	246.52
[Ne VI]	$^2P_{3/2}$–$^2P_{1/2}$	7.6524	126.21	157.93
[Na VI]	$^3P_2$–$^3P_1$	8.6106	138.39	172.15
[Mg VII]	$^3P_1$–$^3P_0$	9.0090	186.51	224.95
[Al VI]	$^3P_0$–$^3{}_1$	9.1160	153.83	190.48
[Mg V]	$^3{}_0$–$^3P_1$	13.5213	109.24	141.27
[Ne V]	$^3P_2$–$^3P_1$	14.3217	97.12	126.21
[Na VI]	$^3P_1$–$^3P_0$	14.3964	138.39	172.15
[Ne V]	$^3P_1$–$^3P_0$	24.3175	97.12	126.21

While the early (broad-band) IR observations found evidence for dust, they were not sufficiently detailed to say anything about the composition of the dust (although carbon was a strong candidate). However IR spectroscopy has been able to reveal spectral features of dust, including silicates and hydrocarbons.

4.2.1 *Nature of the dust*

Several cases exist showing that multiple types of astrophysical grains can form in the ejecta of a single nova. V842 Cen is known to have formed amorphous carbon, silicates, and hydrocarbons (see Gehrz 1990), while QU Vul formed amorphous carbon, SiC, silicates, and hydrocarbons as the ejecta evolved (Gehrz et al. 1992).

V705 Cas was a particularly well-observed dusty nova (Mason et al. 1998; Evans et al. 2003, 2005), and displayed the characteristic deep minimum in the visual light curve. Ground-based IR spectroscopy was obtained for this object, from 1 – 20 μm (Fig. 7). The dust in this nova

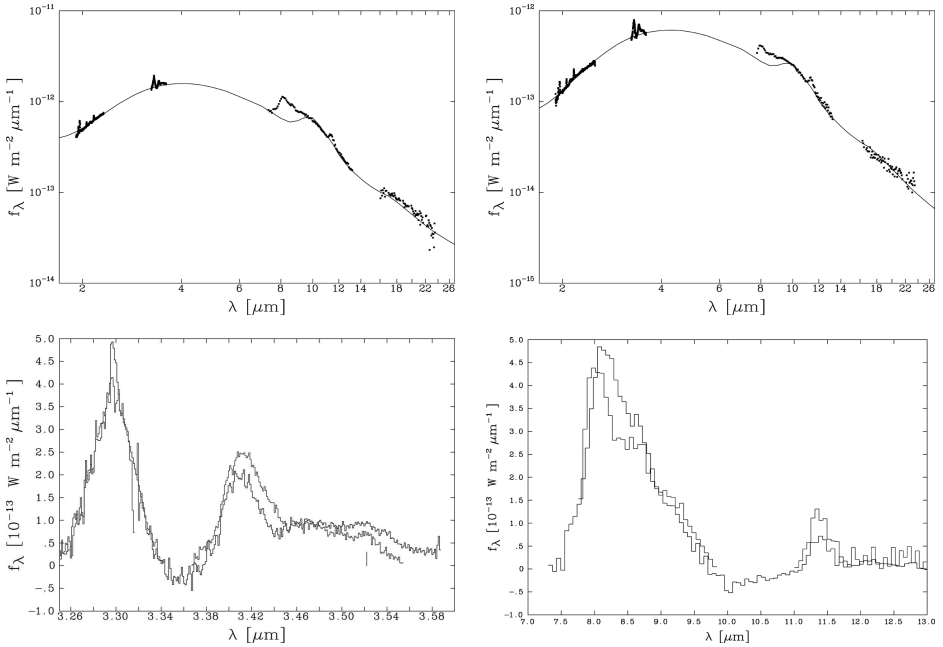

Figure 7. Ground-based IR spectra of V705 Cas, data obtained 253 (left) and 320 (right) days after outburst. Top: SED from 2 – 20 μm; curves are fits using the DUSTY code (Ivezić & Elitzur 1997). Bottom: close-up of the (continuum-subtracted) 3.28 μm and 3.4 μm AIR features, which seem like "noise" in the SEDs in the upper frames. From Evans et al. (2005).

typifies many of the unusual (even anomalous) facets of nova dust, including the condensation of both oxygen- and carbon-rich dust, and the presence of AIR features. The presence of the silicate dust signature at 9.7 μm – normally indicative of an oxygen-rich environment for grain formation – and carbon/AIR emission – indicative of a carbon-rich environment – is at first sight paradoxical and contrary to the "CO paradigm" (see Section 3). The paradox may be resolved by the possibility that, in nova winds, the pre-dust chemistry does not enable CO formation to proceed to saturation, thus allowing the formation of both oxygen- and carbon-rich grain types. Alternatively, there may be significant abundance gradients in the ejected material, for example between the polar plumes and the equatorial ejecta in systems where rotation is high (see Gehrz et al. 1992). Such gradients are also suggested by emission line profiles (see Section 4.1.1 above).

Observations with *Spitzer* have further transformed our view of dust formation and emission in novae. Fig. 8 shows two contrasting novae observed with *Spitzer:* V1065 Cen, which formed primarily silicate dust (Helton et al. 2010), and DZ Cru, which produced amorphous carbon dust and no (or negligible) silicate (Evans et al. 2010). In both cases the presence of nebular and fine-structure lines is evident but in the case of DZ Cru, there are additional broad features due to AIR emission (see below).

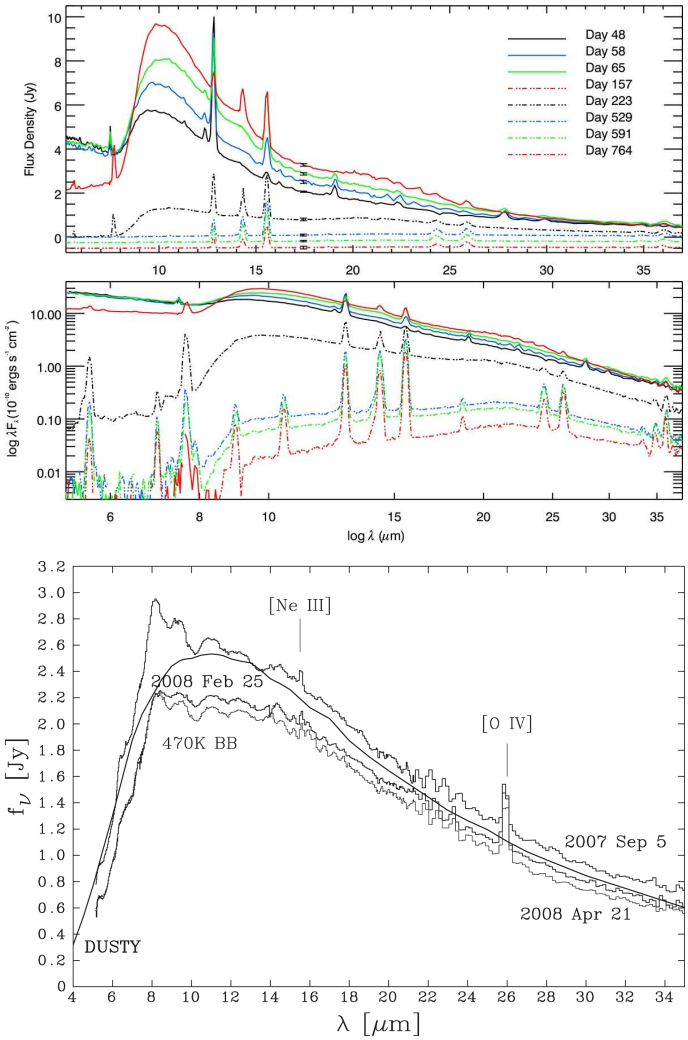

Figure 8. Top: Evolving *Spitzer* spectrum of V1065 Cen, showing a prominent 9.7 μm silicate feature (Helton et al. 2010). Bottom: Evolving *Spitzer* spectrum of DZ Cru, showing strong emission by carbon dust, and the presence of AIR features at 6.45 μm, 7.24 μm, 8.12 μm, 9.29 μm, 10.97 μm and 12.36 μm (Evans et al. 2010).

The broad dust continuum seen in Figs. 7 and 8 is generally attributed to carbon and the presence of AIR features is consistent with this. It is likely that the dust is some form of hydrogenated amorphous carbon (HAC), in which H atoms are attached to the surface of amorphous carbon particles of size ~0.1–1 μm, or polycyclic aromatic hydrocarbons (PAH) in which H atoms are attached to fused aromatic rings. However, as noted by Evans & Rawlings (1994), the lifetime

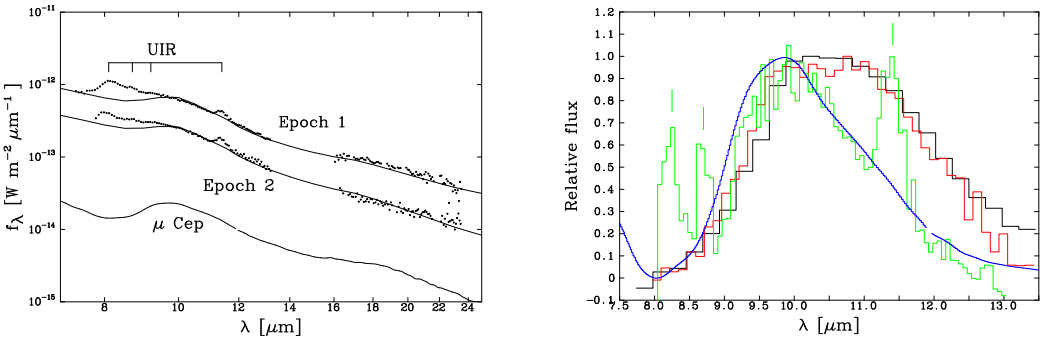

Figure 9. Left: The 9.7 μm silicate feature in V705 Cas; note the weak 18 μm feature. The silicate feature in the red supergiant μ Cep is shown for comparison (Evans et al. 2005). Right: The 9.7 μm silicate feature profile in the novae V1370 Aql (black), V838 Her (red) (Smith et al. 1995) and V705 Cas (green) (Evans et al. 1997, 2005); tick marks are the wavelengths of AIR features in V705 Cas. The silicate feature in the red supergiant μ Cep (blue) is again shown for comparison.

of free-flying PAH molecules in the hard radiation field of novae is extremely short and if such exist in the nova environment, they may originate from the fragmentation of larger HAC particles.

4.2.2 *The silicate features*

The 9.7 μm silicate feature arises from the stretching of the Si–O bond, while the 18 μm feature arises from bending of the O–Si–O bonds. These features do not therefore provide any diagnostic information (e.g. as to whether the silicate is forsterite, Mg_2SiO_4, or fayalite, Fe_2SiO_4), which requires observations at longer wavelengths. However the 9.7 μm feature in V1370 Aql and V838 Her (Gehrz et al. 1984; Smith et al. 1995, respectively) was broader than was the case in V705 Cas and in evolved oxygen-rich stars such as μ Cep, and peaks at longer wavelengths (see Fig. 9). This may be the result of annealing of the silicate in the strong, hard radiation field of the nova.

Note the relative weakness of the 18 μm silicate feature in V705 Cas 320 days after eruption (see Figs. 7 and 9). While this tends to be less prominent than the 9.7 μm feature, it is normally seen in the IR spectra of evolved oxygen-rich stars (cf. the 18 μm silicate feature in μ Cep in Fig. 9). Laboratory work by Nuth & Hecht (1990) suggests that the 18 μm feature is relatively weak in freshly-condensed dust. Their experiments showed that the ratio of the integrated absorption strength of the 9.7 μm feature to that of the 18 μm feature decreases monotonically with increased processing by annealing and oxidation; they suggested that this ratio could therefore be an indicator of the age of the silicate. Thus the relative weakness of the 18 μm feature in the young ejecta of V705 Cas is likely a pointer to the fact that the dust is "fresh", and does indeed form in material ejected in the nova explosion. That the "9.7:18" ratio is a potential indicator of silicate age is consistent with the *Spitzer* IRS observations of V2362 Cyg, in which the 18 μm

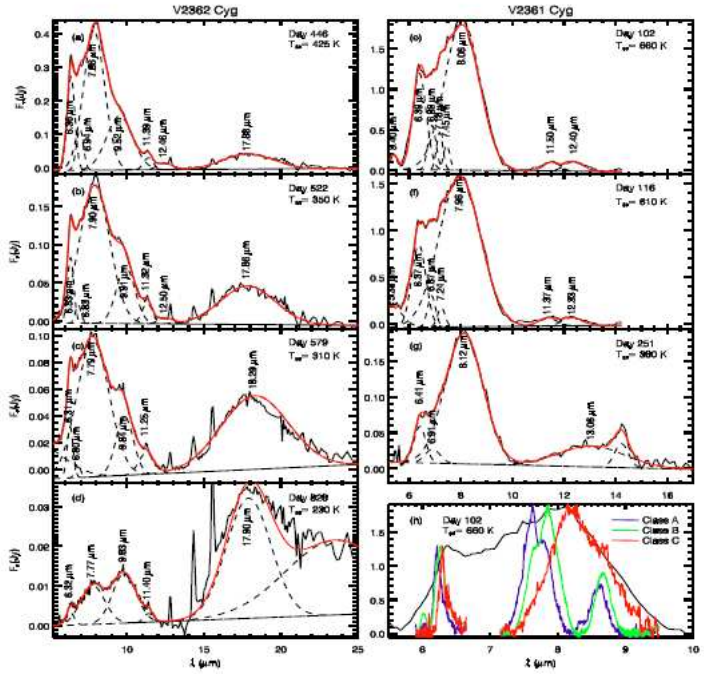

Figure 10. *Spitzer* spectra of two dusty novae (V2362 Cyg, left, and V2361 Cyg, right) displaying AIR features (black curves); in each case a dust continuum has been subtracted. Dashed lines are individual AIR features, represented by Gaussians; red curves are sums of individual components, fitted to the data. From Helton et al. (2011).

feature is initially (446 days after eruption) weak, but increases in strength over the subsequent 400 days (see Fig. 8).

4.2.3 *The AIR features*

AIR emission is frequently seen in novae (such as V842 Cen and V705 Cas; see Fig. 7, lower frames) displaying a deep minimum in the visual light curve; they were first seen in a nova in the case of V842 Cen (Hyland & McGregor 1989). In most astrophysical sources (such as H II regions, planetary nebulae, AGB stars etc.), AIR emission is attributed to PAH molecules (e.g. Tielens 2008), or HAC, although each might represent the extreme ends of a size spectrum of carbonaceous dust grains.

Prominent AIR features are seen at 3.28 μm, 3.4 μm, 6.25 μm, 7.7 μm, 8.6 μm and 11.25 μm[4]

[4]There are other features at other, particularly longer, wavelengths but we do not discuss these here.

and are much broader than emission lines originating in the gas phase. The 3.28 μm feature is attributed to C–H stretch in aromatic (sp^2) hydrocarbons, the 3.4 μm feature to aliphatic (sp^3); the 7.7 μm feature is a blend of several C–C stretching modes, while the 11.25 μm feature is due to C–H out-of-plane bending (see Tielens 2008, for a review).

In novae in which AIR features have been observed, the 3.4 μm feature is much stronger than the 3.28 μm feature (in contrast to the case in other astrophysical sources), while the "7.7" and "11.25" features appear at 8.1 μm and 11.4 μm respectively. In view of the large over-abundance of nitrogen in nova ejecta, the AIR carrier in novae will almost certainly be "contaminated" by N, which will have a significant effect on the properties of the AIR features (see e.g. Evans et al. 2005).

Peeters et al. (2002) have classified AIR features according to their relative strengths and novae AIR features seem to fit Peeters et al.'s "Class C". Objects in this class show no 7.7 μm feature but instead a feature at 8.2 μm; moreover they also display a weak 6.25 μm feature, and an extremely weak 11.25 μm feature; these characteristics are very reminiscent of those seen in novae. In evolved and Herbig Ae/Be stars the wavelength of the "7.7" feature is highly environment-dependent, with a clear dependence of wavelength on the effective temperature of the exciting star (e.g. Peeters et al. 2002; Tielens 2008, and references therein).

Objects in Peeters et al.'s Class C are cool ($\sim$ 5000 K) evolved stars, in stark contrast to the effective temperature of stellar remnant of novae (expected to be $\sim$ 100 000 K). It is curious that novae display AIR features that are reminiscent of cool stars rather than of the hot environment that one would expect. Evans et al. (2010) have suggested that this situation arises because the AIR carrier in novae has only recently been exposed to the hard radiation field of the nova, having been hitherto been protected within the dense clumps needed to form the dust in the first place, thus limiting the photo-processing it has experienced. Alternatively, it may be that only photons having lower energy ever penetrate deeply into the clumps, those of higher energy being converted to lower energy by Lyman and similar scattering at the clump surface, thus mimicking a low temperature environment.

The anomalous AIR features in novae are discussed by Helton et al. (2011), who present a detailed examination of the *Spitzer* spectra of V2361 Cyg and V2362 Cyg (see Fig. 10). In the case of V2362 Cyg the broad features around 9.5 μm and 18 μm may be due to silicates, which are absent in V2361 Cyg (see also above).

An alternative interpretation of the AIR features in novae is given by Kwok & Zhang (2011), who note that the features appear in novae *as the dust is formed*. They too have examined the *Spitzer* spectra of the two dusty novae V2361 Cyg and V2362 Cyg and conclude that the AIR features in novae (and in other sources) arise in complex organic solids which have a mixed $sp^2 - sp^3$ composition. These materials (e.g. coals, kerogens) are present as an insoluble residue in carbonaceous chondrite meteorites and display not only the usual AIR features but also very broad "plateau" features.

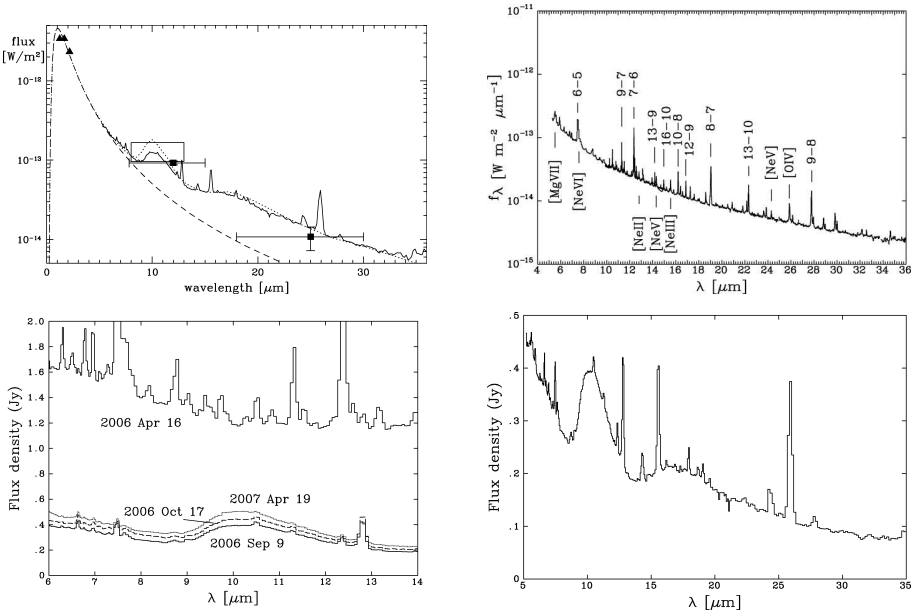

Figure 11. Far-IR observations of RS Oph. Top left: IRAS observations superimposed on *Spitzer* spectrum obtained following 2006 eruption (van Loon 2008). Top right: emisison line spectrum during the 2006 eruption, as observed by *Spitzer*. Botton frames: silicate dust in the environment of RS Oph. *Spitzer* data from Evans et al. (2007b,c).

5. The recurrent novae

A nova system that is observed to undergo a second eruption becomes a recurrent nova: the difference between classical and recurrents is the selection effect that a recurrent is a classical that has undergone more than one eruption (see Anupama 2008; Evans et al. 2008, for recent reviews). Few recurrents are known, and those that are known form a very heterogeneous group. Other potential recurrents have been identified, on the basis of the nature of their secondaries and the amplitude at outburst (see e.g. Weight et al. 1994; Darnley et al. 2012, and references therein).

Since the widespread availability of IR in the 1970s there have been few RN eruptions and so few IR observations of RNe in outburst exist, especially longward of 3 μm. The first extensive IR observations were those of the 1985 eruption of RS Oph (Evans et al. 1988). In recent years, observations longward of 3 μm of the eruptions of RS Oph (2006) and T Pyx (2011) have been obtained and we describe these here.

5.1 RS Oph (2006)

Spitzer IRS observations of the 2006 eruption of RS Oph are described by (Evans et al. 2007b,c, see Fig. 11). An observation 62.5 days after outburst shows a rich emission line spectrum (includ-

ing fine-structure and coronal lines) super-imposed on a free-free continuum (Evans et al. 2007b). The presence of coronal lines is not unexpected as the ejected material from the 2006 eruption runs into and shocks the red giant wind (Bode & Kahn 1985). However, unlike the case for classical novae, it is not straight-forward to use the fine-structure and coronal lines to determine abundances as the observed lines are a mix of shocked wind and ejecta. A first requirement is the determination of abundances in the wind, either by determining abundances in the atmosphere of the red giant (e.g. Pavlenko et al. 2008), or in the red giant wind (e.g. by analysing the IR spectrum of the flash-ionised wind; Evans et al. 2007a). Analysis of the coronal lines after the 2006 eruption indicates that there are two regions in the emitting gas, with temperatures 1.5×10^5 K and 9×10^5 K.

As the free-free emission declined the *Spitzer* observations of RS Oph revealed a major surprise: a substantial amount of silicate dust in the circumstellar environment (see Fig. 11, from Evans et al. 2007c). Note the strong 18 μm silicate feature, which indicates that the dust observed cannot be freshly condensed as this would show a weak 18 μm feature (see above; Nuth & Hecht 1990). The relatively strong 18 μm feature indicates that the dust is "old", and that there is a substantial amount of dust in the environment of the RS Oph binary that is completely oblivious to the nova eruption.

RS Oph was observed in the course of the IRAS survey in 1983, and *Spitzer* observations that show the silicate emission in the aftermath of the 2006 eruption are super-imposed on the IRAS data in Fig. 11 (van Loon 2008). That the IRAS data were obtained before either the 1985 or the 2006 eruptions reinforces the fact that the dust is pre-existing, and a constant feature of the RS Oph system; a substantial fraction of the red giant wind must (as noted by Woodward et al. 2008) be "blissfully unaware" of the violent events that occur near it. This silicate dust presumably originates in the wind of the red giant star in the RS Oph binary system and its discovery has major implications for the evolution of the underlying binary, and for mass-loss from the system. Given that the 2006 observations were the the first to see the silicate, it is not known whether the 2006 eruption (and indeed previous eruptions) affected the amount of dust (or indeed its nature) in the circumstellar environment; observations of the next outburst in the same wavelength range will be valuable to see if the eruptions have any effect on the dust.

5.2 T Pyx (2011)

T Pyx was the first nova to be identified as a recurrent, and has undergone 6 nova eruptions since 1890. Its most recent eruption (2011) was observed with *Spitzer* and *Herschel*. The SED 26.2 days after the eruption is shown in Fig. 12 (black curve) and is consistent with emission by dust longward of $\sim 50\,\mu$m. Evans et al. (2012) conclude that the emission is due to pre-existing dust in the environment of T Pyx, the result of the sweeping up of interstellar dust, either by winds or by material ejected in the course of previous recurrent nova eruptions. T Pyx is the first nova in which an "infrared echo" – postulated by Bode & Evans (1980) to account for the dust emission – has been observed. If this is indeed the case the reverberation effect means that the far-IR emission should be detectable for several years after the 2011 eruption (Evans et al. 2012).

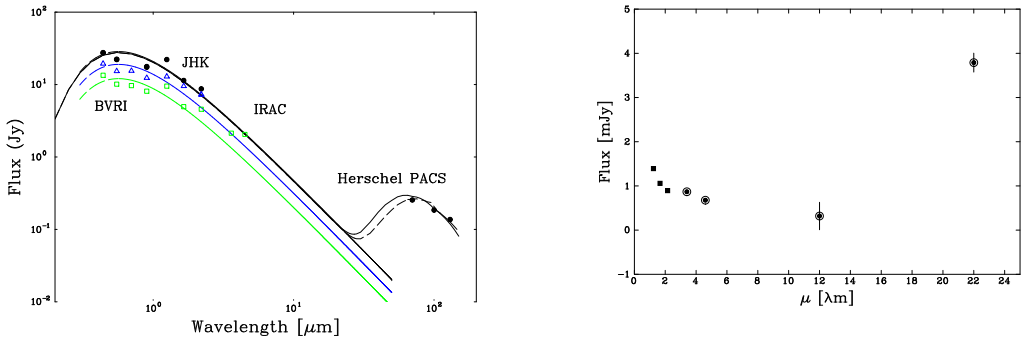

Figure 12. Left: SED of T Pyx following the 2011 eruption. Ground-based IR data from Mt Abu and SMARTS (Walter et al. 2004); mid-IR data from *Spitzer* and *Herschel*. Spectral fits for 9000 K blackbody illuminating pre-existing circumstellar dust. From Evans et al. (2012). Right: inter-outburst SED, based on 2MASS and WISE sky surveys. See text for details.

T Pyx is detected in the 2MASS (Skrutskie et al. 2006) and WISE (Wright et al., 2010) sky surveys and the SED based on these is also shown in Fig. 12. There seems to be an excess at 22 μm, although observations at other wavelengths would be valuable to confirm this. If so, the quiescent data seem consistent with the presence of cool dust in the environment of T Pyx between outbursts.

6. Future prospects

6.1 The Stratospheric Observatory for Infrared Astronomy (SOFIA)

The US/German Stratospheric Observatory for Infrared Astronomy (SOFIA), a joint project of NASA and the Deutsches Zentrum für Luft und Raumfahrt (DLR), is a gyro-stabilized 2.5-meter clear aperture IR telescope mounted in the aft fuselage of a Boeing 747-SP aircraft (see Fig. 13 and Young et al., 2012). The observatory will make sensitive IR spectroscopic measurements at wavelengths from 0.3 μm to 1.6 mm. SOFIA, which will fly until the mid-2030s, will be a key facility for chemical/dynamical studies of classical and recurrent novae. The characteristics of the initial suite of spectrometers are summarized in Table 3.

SOFIA will fly at altitudes as high as 45,000 feet (13.7 km), above 99.8% of the remaining atmospheric water vapour. At this altitude, the precipitable atmospheric water typically has a column depth of less than 10 μm, 20–100 times lower than at good terrestrial sites. The atmospheric transmission averages 80% or better across SOFIA's wide wavelength range.

SOFIA has several features that will make it an outstanding facility for observing nova explosions (Gehrz et al. 2009):

Figure 13. NASA's SOFIA infrared observatory over Southern California's high desert on July 13, 2010 during flight testing in preparation for the Early Science Program. Image courtesy of the NASA Dryden Flight Research Center Photo Collection.

Table 3. SOFIA's First Generation Spectrometer Summary[a]

Name[b]	Description	PI	Institution	Wavelengths (μm)	Spectral Resolution
FORCAST	Mid-Infrared Camera and Grism Spectrometer	T. Herter	Cornell	5–40	90–1200
GREAT	Heterodyne Spectrometer	R. Güsten	MPIfR	60–240	106–108
FLITECAM	Near-Infrared Camera and Grism Spectrometer	I. McLean	UCLA	1–5	900–1700
EXES	Mid-Infrared Spectrometer	M. Richter	UC Davis	5–28	3000, 104, 105
FIFI-LS	Integral Field Far-Infrared Spectrometer	A. Krabbe	U Stuttgart	42–210	1000–3750

(a) Details available at http://www.sofia.usra.edu/Sciecnce/instruments;

(b) Earliest availability for GI programmes: Cycle 1 (2013): FORCAST with grisms, and GREAT; Cycle 2 (2014): EXES and FIFI-LS.

1. Its mobility – the ability to travel to any airfield that can handle a 747 on short notice – will facilitate the timely monitoring of the temporal development of nova events anywhere in the sky. Coverage of the entire development of a single nova requires observational cadences that cover events that develop on time-scales of days, weeks, and months.
2. The spectroscopic capabilities of the instruments summarised in Table 3 will enable the recording of many forbidden lines obscured by the atmosphere from ground-based observatories and unavailable to the spectrometers of other space missions. An assessment of the strengths of these lines is necessary to determine accurate elemental abundances in nova ejecta.
3. High resolution spectroscopy of these lines will provide a powerful probe of the physical conditions (e.g., density and temperature), ionisation state, energetics, mass, and kinemat-

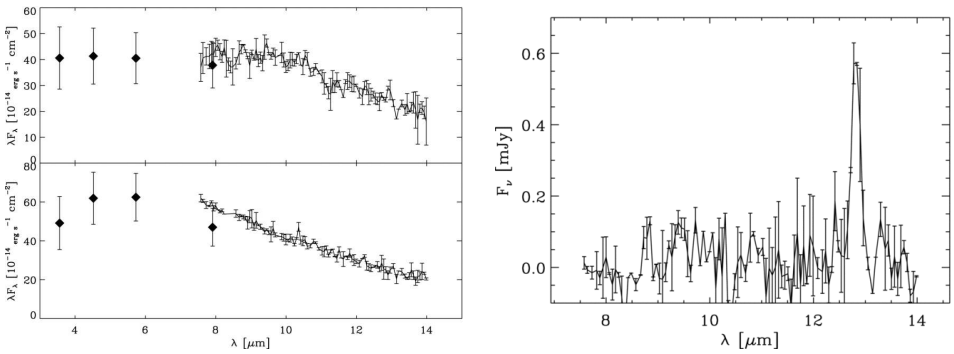

Figure 14. Left: IR SEDs for two M31 novae, M31N 2006-09c (upper panel) and M31N 2006-10a (lower panel); note the IR excess, due to emission by dust, in M31N 2006-10a. Right: *Spitzer* IRS spectrum of M31N 2007-11e, showing the [Ne II]12.81 μm fine-structure line. From Shafter et al. (2011).

ics of the ejected gas through studies of the atomic fine structure lines of [O I] (63 μm and 145 μm), [O III] (52 μm, 88 μm), [O IV] (25.9 μm), [C II] (158 μm), [S I] (26 μm), [Si II] (34 μm), and [S III] (18.7 μm); see also Tables 1 and 2. Furthermore, many forbidden lines of neon, whose abundance is an indicator of progenitor mass and WD type, lie in obscured atmospheric bands that can be observed by SOFIA.

4. SOFIA is unique in that the spectral coverage and resolution of its spectrometers is perfect for assaying the detailed mineralogy of nova dust, a task that was only cursorily begun by *Spitzer* IRS observations. In particular it will be possible to make a detailed study of silicate crystallinity (see e.g. Fabian et al. 2002; Molster et al. 2002) in novae that produce silicate dust (see Section 4.2), and of AIR features at wavelengths not reached by the *Spitzer* IRS (see Tielens 2008). Of particular interest are the far-IR AIR features expected to be associated with the low-lying vibrational modes corresponding to the "drum-head" modes of large PAH molecules.

SOFIA observing time for General Investigator (GI) programmes will be competed for and awarded on annual cycles. Proposal awards for Cycle 1 were announced in late August 2012 and observations will occur during 2013 January – 2013 December. Cycle 2 proposals will be solicited in 2013 April, and will be harvested in 2013 June for flight during 2014 January – 2014 December. By 2014, the SOFIA programme expects to be doing up to $\sim$ 1000 hours of science observations per year (12% of the total time). Observing opportunities will be announced from time to time on the SOFIA website at www.sofia.usra.edu.

6.2 The James Webb Space Telescope

NASA's James Webb Space Telescope (JWST; Gardner et al. 2006) is now working to a 2018 launch, with an expected ten year lifetime. It will have two spectrometers capable of following the temporal spectral development of classical and recurrent novae. The near-IR spectrometer

(NIRSPEC) will cover 1–5 μm with spectral resolutions of $R \sim 100 - 3000$, and the mid-IR instrument (MIRI) will cover 5–28 μm at $R \sim 100 - 3000$. These instruments have integral field units and are not especially efficient for viewing single point sources like Galactic novae.

However, the very high sensitivity of these instruments make them well suited for discovering nova populations in external galaxies. Their potential in this regard is well illustrated by *Spitzer* InfraRed Array Camera (Fazio et al. 2004) and IRS observations of novae in M31 by Shafter et al. (2011). Fig. 14 shows the IR SEDs of the two novae M31N 2006-09c and 2006-10a. The IR excess, peaking in λf_λ at $\sim 4\,\mu$m, is evident in the case of M31N 2006-10a; this nova had $t_2 \sim 50$ days (in the R band), characteristic of dust-forming novae in the Galaxy. The nova M31N 2007-11e showed clear evidence for emission in the [Ne II]12.81 μm fine-structure line, the Humphreys$-\alpha$ 12.37 μm line being very weak or absent. While the presence of the [Ne II] line is a necessary, but not sufficient, condition for classification as a neon nova, there is clearly the potential to undertake unbiassed population studies of extragalactic novae with JWST. This is all the more so as extinction – even less well known in extragalactic environments than it is in the Galaxy – is a relatively minor irritant in the IR.

On the other hand, viewing constraints imposed by the L-2 orbit will likely prevent JWST from making timely target of opportunity observations of many novae. The spectral coverage limits JWST nova observations to wavelengths shorter than 28 μm.

6.3 Other facilities

A number of very large aperture telescopes capable of 3–25 μm ground-based follow-up of nova events have recently come into operation or will soon begin full-time operations. These include 8–10 m telescopes such as Gemini (Roche et al. 2001), VLT (Merkle & Schneermann 1986), Keck (Nelson 1989), and the Large Binocular Telescope (LBT; Hill 1997). In addition to their sensitive spectroscopic capabilities, several of these telescopes are equipped with laser guide stars and adaptive optics that can achieve spatial resolutions of $0.04 - 0.10''$ at wavelengths $> 3\,\mu$m that may enable them to image young nova ejecta in some cases.

Future very large ground-based giant segmented mirror telescope (GSMTs) such as the Giant Magellan Telescope (GMT; Johns 2004), the Thirty Meter Telescope (TMT; Nelson 2008), and the European Extremely Large Telescope (E-ELT; Monnet 2007) will extend the spectroscopic and imaging capabilities even further.

Prospective observers should consult the websites of all of these facilities for information about progress and observing opportunities

7. Concluding remarks

Over the past ~ 30 years IR observations have proven to be pivotal in advancing our understanding of the nova phenomenon, and pan-chromatic observations – combining IR with optical, UV

and X-ray observations – has been especially effective (as in the case of RS Oph for example). It is highly desirable that future novae (both classical and recurrent) continue to be observed over as broad a wavelength range as possible, particularly as systematic observations of extragalactic novae will soon be a real possibility.

While great strides have been made in recent years, there remain some substantial gaps in our understanding (and IR observational coverage) of novae. For example we have little IR spectroscopy of molecules in novae, with CO being the only molecule securely detected in the IR to date (see above, Evans & Rawlings 2008, and references therein); molecular rotational/vibrational transitions can provide crucial information about isotope ratios, critical to TNR modelling.

However we can expect that, in the next decade, SOFIA will fill in the IR spectroscopic gaps tantalisingly opened up by *Spitzer*. In particular fine-structure lines beyond the *Spitzer* IRS range will become accessible, particularly in old, low density, remnants (such as DQ Her). Furthermore, it will be possible for the first time to undertake a detailed mineralogical study of nova dust, particularly nova silicates, and the way in which the silicate evolves as it is processed.

To paraphrase Winston Churchill: *Spitzer* "is not the end. It is not even the beginning of the end. But it is, perhaps, the end of the beginning".

Acknowledgements

RDG was supported by NASA and the United States Air Force.

References

Anupama G. C., 2008, in Evans A., et al., eds, RS Ophiuchi (2006) and the Recurrent Nova Phenomenon, ASP Conf. Series, 401, p. 31
Asplund M., Grevesse N., Sauval A. J., Scott P., 2009, ARAA, 47, 481
Banerjee D. P. K., Ashok N., 2012, BASI, 40, 243
Bath G. T., 1978, MNRAS, 182, 35
Bath G. T., Harkness R. P., 1989, in Bode M. F., Evans A., eds, Classical Novae, first edition, Wiley, Chichester, p. 61
Bode M. F., Evans A., 1980, A&A, 89, 158
Bode M. F., Evans A., 2008, eds, Classical Novae, second edition, Cambridge University Press
Bode M. F., Kahn F., 1985, MNRAS, 217, 205
Darnley M. J., Ribeiro V. A. R. M., Bode M. F., Hounsell R. A., Williams R. P., 2012, ApJ, 746, 61
de Graauw T., et al., 1996, A&A, 315, L49
Ennis D., Becklin E. E., Beckwith S., Elias J., Gtley I., Matthews K., Neugebauer G., 1977, ApJ, 214, 478
Evans A., Bode M. F., O'Brien T. J., Darnley M. J., 2008, eds, RS Ophiuchi (2008) and the Recurrent Nova Phenomenon, Astronomical Society of the Pacific Conference Series, volume 401
Evans A., Callus C. M., Albinson J. S., Whitelock P. A., Glass I. S., Carter B., Roberts G., 1988, MNRAS, 234, 755
Evans A., Geballe T. R., Rawlings J. M. C., Eyres S. P. S., Davies J. K., 1997, MNRAS, 292, 192

Evans A. et al., 2003, AJ, 1981
Evans A., Tyne V. H., Smith O., Geballe T. R., Rawlings J. M. C., Eyres S. P. S., 2005, MNRAS, 360, 1483
Evans A., Rawlings J. M. C., 1994, MNRAS, 269, 427
Evans A., Rawlings J. M. C., 2008, in Bode M. F., Evans A., eds, Classical Novae, p. 308, second edition, Cambridge University Press
Evans A., et al., 2003, AJ, 126, 1981
Evans A., et al., 2007a, MNRAS, 374, L1
Evans A., et al., 2007b, ApJ, 663, L29
Evans A., et al., 2007c, ApJ, 671, L157
Evans A., et al., 2010, MNRAS, 406, L85
Evans A., et al., 2012, MNRAS, 424, L69
Fabian D., Henning T., Jäger C., Mutschke H., Dorschner J., Wehrhan O., 2001, A&A, 378, 184
Fazio G. G., et al. 2004, ApJS, 154, 10
Ferland G. J., Shields G. A., 1978a, ApJ, 224, L15
Ferland G. J., Shields G. A., 1978b, ApJ, 226, 172
Ferland G. J., Williams R. E., Lambert D. L., Slovak M., Gondhalekar P. M., Truran J. W., 1984, ApJ, 281, 194
Ferland G. J., Korista K. T., Verner D. A., Ferguson J. W., Kingdon J. B., Verner E. M., 1998, PASP, 110, 761
Gardner J. P., et al., 2006, Space. Sci. Rev., 123, 485
Gehrz R. D., 1988, ARAA, 26, 377
Gehrz R. D., 1990, in eds Cassatella A., Viotti R., eds, Physics of Classical Novae, IAU Coll. 122, Springer-Verlag, p. 138
Gehrz R. D., 2008, in Bode M. F., Evans A., eds, Classical Novae, second edition, Cambridge University Press, p. 167
Gehrz R. D., Ney E. P., 1987, Proc. Nat. Acad. Sci., 84, 6961
Gehrz R. D., Becklin E. E., de Pater I., Lester D. F., Roellig T. L., Woodward C. E., 2009, Adv. Space Res., 44, 413
Gehrz R. D., Grasdalen G. L., Hackwell J. A., 1985, ApJ, 298, L47
Gehrz R. D., Grasdalen G. L., Hackwell J. A., Ney E. P. 1980, ApJ, 237, 855
Gehrz R. D., Hackwell J. A., Briotta D., 1976, BAAS, 8, 509
Gehrz R. D., Ney E. P., Grasdalen G. L., Hackwell J. A., Thronson H. A., 1984, ApJ, 281, 303
Gehrz R. D., Jones T. J., Woodward C. E., Greenhouse M. A., Wagner R. M., Harrison T. E., Hayward T. L., Benson J., 1992, ApJ, 400, 671
Gehrz R. D., Truran J. Y., Williams R. E., Starrfield S., 1998, PASP, 110, 3
Gehrz R. D., et al., 2007, Rev. Sci. Instr., 78, 011302
Gehrz R. D., et al., 2008, ApJ, 672, 1167
Geisel S. L., Kleinmann D. E., Low F. J., 1970, ApJ, 161, L101
Greenhouse M. A., Grasdalen G. L., Woodward C. E., Benson J., Gehrz R. D., Rosenthal E., Strutskie M. F., 1990, ApJ, 352, 307
Helton L. A., et al., 2010, AJ, 140, 1347
Helton L. A., Evans A., Woodward C. E., Gehrz R. D., 2011, in Joblin C., Tielens A. G. G. M., eds, PAHs and the Universe, EAS Publication Series, Vol. 40, p. 407
Helton L. A., Gehrz R. D., Woodward C. E., Wagner R. M., Vacca W. D., Evans A., Krautter J., Schwarz G. J., Shenoy D. P., Starrfield S., 2012, ApJ, 755, 37
Hill J. M. 1997, in Proc. of the SPIE 2871, p. 57
Houck J. R., et al., 2004, ApJS, 154, 18
Hyland A. R., McGregor P., 1989, in Allamandola, L. J., Tielens A. G. G. M., eds, Interstellar Dust, IAY

Symp. 135, NASA Conference publication, p. 101
Ivezić Z., Elitzur M., 1997, MNRAS, 287, 799
Johns M. W. 2004, Proc. of the SPIE 5382, 85
José J., Shore S. N., 2008, in Bode M. F., Evans A., eds, Classical Novae, second edition, Cambridge University Press, p. 121
Kessler M. F., et al., 1996, A&A, 315, L27
Krautter J., 2008, in Bode M. F., Evans A., eds, Classical Novae, second edition, Cambridge University Press, p. 232
Kwok S., Zhang Y., 2011, Nature, 479, 80
Lutz D., 2002, http://www.mpe-garching.mpg.de/iso/linelists/FSlines.html
Lyke J. E. et al., 2001, AJ, 122, 3305
Lyke J. E. et al., 2003, AJ, 126, 993
Lynch D. K., et al., 2006, ApJ, 638, 987
Lynch D. K., et al., 2008, AJ, 136, 1815
McLaughlin D. B., 1935, Publ. AAS, 8, 145
Martin P. G., 1989a, in Bode M. F., Evans A., eds, Classical Novae, first edition, Cambridge University Press, p. 93
Martin P. G., 1989b, Bode M. F., Evans A., eds, Classical Novae, first edition, Wiley, Chichester, p. 113
Mason C. G., Gehrz R. D., Woodward C. E., Similowitz J. B., Hayward T. L., Houck J. R., 1998, ApJ, 494, 783
Merkle F., Schneermann M., 1986, Sterne und Weltraum 25, 460
Mitchell R. M., Evans A., 1984, MNRAS, 209, 945
Mitchell R. M., Evans A., Albinson J. S., 1986, MNRAS, 221, 663
Molster F. J., Waters L. B. F. M., Tielens A. G. G. M., 2002, A&A, 382, 222
Monnet G. J. 2007, Highlights of Astronomy 14, 524
Morriset C., Stasińska G., Peña M., 2005, MNRAS, 360, 499
Nelson J. 1989, American Scientist 77, 170.
Nelson J. 2008, Proc. of the SPIE, 6986, 2
Ney E. P., Hatfield B. F., 1978, ApJ, 219, L111
Nuth J. A., Hecht J. H., 1990, Ap. Sp. Sci., 1990, 163, 79
Pavlenko Ya. V., Evans A., Kerr T., Yakovina L., Woodward C. E., Lynch D., Rudy R., Pearson R. L., Russell R. W., 2008, A&A, 485, 541
Payne-Gaposchkin C. E., 1957, The Galactic Novae, North Holland
Peeters E., Hony S., Van Kerckhoven C., Tielens A. G. G. M., Allamandola L. J., Hudgins D. M., Bauschlicher C. W., 2002, A&A, 390, 1089
Roche P., et al., 2001, Astronomische Gesellschaft Abstract Series 18, 224
Rushton M. T., Evans A., Eyres S. P. S., van Loon J. Th., Smalley B., 2008, MNRAS, 386, 289
Salama A., Evans A., Eyres S. P. S., Leech K., Barr P., Kessler M. F., 1996, A&A, 315, L209
Salama A., Eyres S. P. S., Evans A., Geballe T. R., Rawlings J. M. C., 1999, MNRAS, 304, L20
Schwarz G. J., 2002, ApJ, 577, 940
Schwarz G. J. et al., 2007, AJ, 134, 516
Seaquist E. R., Bode M. F., 2008, in Bode M. F., Evans A., eds, Classical Novae, second edition, Cambridge University Press, p. 141
Shafter A. W., Bode M. F., Darnley M. J., Misselt K. A., Rubin M., Hornoch K., 2011, ApJ, 727, 50
Shore S. N., Gehrz R. D., 2004, A&A, 417, 695
Shore S. N., Starrfield S., Gonzalez-Riestra R., Hauschildt P. H., Sonneborn G., 1994, Nature, 369, 539
Skrutskie M. F., et al., 2006, AJ, 131, 1163
Smith C. H., Aitken D. K. Roche P. F., Wright C. M., 1995, MNRAS, 277, 259

Smith N., Gehrz R. D., Goss W. M., 2001, AJ, 122, 2700
Smith N., Gehrz R. D., Campbell R., Kassis M., Le Mignant D., Kuluhiwa K., Filippenko A. V., 2011, MNRAS, 418, 1959
Starrfield S., Iliadis C. Hix W. R., 2008, in Bode M. F., Evans A., eds, Classical Novae, second edition, Cambridge University Press, p.77
Tielens A. G. G. M., 2008, ARAA, 46, 289
van Loon J. Th., 2008, in Evans A., et al., eds, RS Ophiuchi (2006) and the Recurrent Nova Phenomenon, ASP Conference Series volume 401, p. 90
Wallerstein, G., 2008, in Evans A., et al., eds RS Ophiuchi (2006) and the Recurrent Nova Phenomenon, ASP Conference Series volume 401, p. 41
Walter F. M., Field-Pollatou A., Miner J., Nyquist R., Howell S. B., Stringfellow G. S., 2004, AAS, 36, 1618
Weight A., Evans A., Naylor T., Wood J. H., Bode M. F., 1994, MNRAS, 266, 761
Werner M. W., et al., 2004, ApJS, 154, 309
Woodward, C. E., Helton, L. A., Evans, A., van Loon, J. Th., Gehrz, R. D., et al., 2008, in Evans A., Bode M. F., O'Brien T. J., Darnley M. J., eds, RS Ophiuchi (2006) and the Recurrent Nova Phenomenon, Astronomical Society of the Pacific Conference Series volume 401, p. 260
Wright E. L., et al., 2010, AJ, 140, 1868
Young E. T., et al., 2012, ApJ, 749, L17